CARBON 47 (2009) 675–682

available at www.sciencedirect.com

ScienceDirect

journal homepage: www.elsevier.com/locate/carbon

Cap removal and shortening of double-walled and very-thin multi-walled carbon nanotubes under mild oxidative conditions

Riccardo Marega[a], Gianluca Accorsi[c], Moreno Meneghetti[b], Andrea Parisini[d], Maurizio Prato[a], Davide Bonifazi[a,e,*]

[a]Center of Excellence for Nanostructured Materials, CENMAT, Dipartimento di Scienze Farmaceutiche, INSTM UdR di Trieste, Università degli Studi di Trieste, Piazzale Europa 1, 34127 Trieste, Italy

[b]Dipartimento di Scienze Chimiche, Università degli Studi di Padova, 35131 Padova, Italy

[c]Molecular Photoscience Group – Istituto per la Sintesi e la Fotoreattività (ISOF), Consiglio Nazionale delle Ricerche (CNR), Via Gobetti 101, Bologna, Italy

[d]Istituto per la Microelettronica e i Microsistemi del CNR, 40136 Bologna, Italy

[e]Chemistry Department, University of Namur, Rue de Bruxelles 61, 5000 Namur, Belgium

ARTICLE INFO

Article history:
Received 13 April 2008
Accepted 30 October 2008
Available online 27 November 2008

ABSTRACT

Homogeneous carbon-based materials were prepared for endohedral functionalization starting from carbon nanotubes (CNT) samples mainly containing double-walled and very-thin multi-walled CNTs. Comprehensive structural characterization of end-opened and shortened CNTs, which were prepared under mild oxidative conditions using dilute aqueous H_2O_2 solutions, is reported. 90% of the 400 measured nanotubes were shorter than 1 μm with an average value of about 500 nm. TEM observations have confirmed the shortening and opening of the end caps. TGA analysis and Raman spectroscopy showed a reduced impurity content after the oxidation treatment.

© 2008 Elsevier Ltd. All rights reserved.

1. Introduction

Since the landmark paper by Iijima, multi-walled nanotubes (MWCNTs) [1] and single-walled nanotubes (SWCNTs) [2,3] have drawn a great attention from the scientific community for their great potential in a large number of different technological fields, such as high-strength composites, [4] photovoltaic cells, [5–7] electronic devices, [8] hydrogen molecular storages, [9] and biotechnology [10–13]. In particular, carbon nanotubes (CNTs) have been proposed as nanometer-scale scaffolds for DNA recognition and protein biosensors [14–18], as bioseparators and biocatalysts [19], and as well as biocompatible nanocarriers of biologically-active molecules [20–25]. Thus, CNTs modified with appropriate external and/or internal appends could be regarded as potential radiotracers and nanovehicles for both *in vitro* and *in vivo* imaging [26,27]. Despite their great potentials, CNTs have shown some severe restrictions regarding the manipulation of the raw materials: first, the hydrophobic properties of the graphene network are exalted by the high surface area of the nanotubes, causing extraordinary inter-tube Van der Waals interactions (and thus very limited solubility of the unmodified materials in the common organic solvents and aqueous solutions); [28] secondly, pristine samples of CNTs are structurally very inhomogeneous (i.e., different chirality, length, and diameter) and they contain large quantities of metallic and

* *Corresponding author:* Address: Chemistry Department, University of Namur, Rue de Bruxelles 61, 5000 Namur, Belgium. Fax: +32 81 725433.
E-mail address: davide.bonifazi@fundp.ac.be (D. Bonifazi).
0008-6223/$ - see front matter © 2008 Elsevier Ltd. All rights reserved.
doi:10.1016/j.carbon.2008.10.049

Samsung Ex. 1011, Page 1 of 8
Samsung Electronics Co., Ltd., et al. v. Molecular Rebar Design, LLC
IPR2025-00358

carbonaceous impurities, which greatly differ by the production technology (arc discharge, [3] laser ablation, [29] chemical vapour deposition, [30] and HiPco processes [31]). Impurity content and dimensional variance are thus the two major parameters characterizing the heterogeneity of this material. The controlled growth of these carbonaceous structures on solid support has revealed to produce homogeneous CNTs samples, but its recent development is still limited at the mg scale.

Two main approaches have been widely investigated so far: covalent and non-covalent modifications [32]. Amongst, the common derivatization reactions, oxidative reactions seem able to reduce the heterogeneity level of the pristine CNTs and overcome most of the aforesaid limitations. So far, several oxidation reactions have been used to generate shortened SWCNTs bearing carboxylic moieties, [33] to remove or reduce the amount of catalytic and carbonaceous particles adsorbed onto their sidewall [33–39]. Moreover, various oxidative treatments have been also developed to open the CNTs' ends by oxidizing the fullerene-like end tips, generating open-shell nanotube [40–42]. In order to achieve one or more of these goals, two main oxidation strategies have been extensively studied: with liquid or with gaseous reagents under different combinations of temperature and time. As liquid reagents, many solutions of HNO_3, H_2SO_4, or H_2O_2 at different concentrations, proportions, and mixtures have been used [33,43–45]. Heat treatments, under different atmospheres (wet and dry air, CO_2 and inert gas), have been mainly applied to purify raw materials [35,41]. The modifications generated onto the CNT frameworks have been recently rationalized by means of Raman spectroscopy investigations. Following the magnitude of the D-band feature at 1330 cm^{-1}, as the oxidizing conditions get stronger, the number of defects (related to the presence of sp^3-hydridized carbon atoms) proportionally increase, thus affecting the probability of length shortening [46]. Moreover, comparative study on gas- and liquid-based oxidative treatments on SWCNTs allowed to conclude that, unlike liquid-phase reactions, the gas-phase processes preferentially oxidizes the SWCNTs without introducing sidewall defects [34]. On the basis of high degree of available information and the different results obtained for the oxidation of CNTs, we used mild oxidative conditions to treat CNT samples containing DWCNTs and Vt-MWCNTs, in order to see if shortened, homogeneous materials end-opened CNTs could be obtained without significant material loss. The structural properties have been fully characterized *via* Thermogravimetric analysis (TGA), Raman spectroscopy, low-and high-resolution Transmission Electron Microscopy (LR- and HR-TEM) and Atomic Force Microscopy (AFM). In particular, a statistical analysis of the structural properties, as evaluated from AFM measurements, shows that 90% of the 400 measured units were shorter than 1 μm with an average value of about 500 nm.

2. Experimental

2.1. General

Reagents and solvents were purchased reagent grade and used without further purification; H_2O_2 30 wt% (PERDROGEN®) was purchased from Riedel de Haen, CNTs and p-CNTs (purified CNTs), both produced by the Catalytic Carbon Vapor Deposition (CCVD) process, were purchased from Nanocyl (respectively, Nanocyl®-2100 and Nanocyl®-2101). Both samples revealed to contain a considerable amount of Vt-MWCNTs. In a typical experimental procedure, 100 mg of CNTs were dispersed in 100 ml of a 15% H_2O_2 solution. The resulting suspensions were heated at 100 °C for 3 h under moderate stirring; afterwards the reaction mixtures were quickly diluted in 1.5 L of H_2O, in order to quench the oxidizing reaction. The diluted suspensions were then filtered under reduced pressure through Millipore GTTP 0.2 μm filter with the aim of separate the black precipitates (***sh*-CNTs**) from the transparent acidic solutions. The ***sh*-CNTs** on the filter were washed with 0.5 L of water and with some MeOH to facilitate their drying. Dried products were dispersed in 50 ml of 2*N* HCl solutions via sonication (1 min) and then stirred at r.t. for 10 min, before being diluted with 50 ml of H_2O and filtered in the same conditions (Millipore GTTP 0.2 μm filter) as those used before yielding 48.3 mg (starting from 2100 grade) or 66.3 mg (starting from 2101 grade) of ***sh*-CNTs**. These amounts of ***sh*-CNTs** were successively placed in an oven at 450 °C under external air purge for 45 min, giving 23.0 and 42.2 mg of ***ox*-CNTs**, respectively.

2.2. Instrumentation and samples preparation for the analysis

All the thermogravimetric analysis (TGA) were performed with a *TGA Q500* instrument manufactured by TA instruments (Italy), under a N_2 flow of 50 ml min^{-1} following this method: equilibration from room temperature to 100 °C in 6 min, isothermal heating at 100 °C for 30 min, then thermal ramp from 100 °C to 1000 °C in 90 min (heating rate of 10 °C min^{-1}). All the TEM images were obtained from the deposition onto Nickel grids (with carbon layer coating, 200 mesh) of dispersions (approximately 1 mg ml^{-1}) of ***pristine*-CNTs** (both types), ***sh*-CNTs**, and ***ox*-CNTs** in 1,2-dichlorobenzene; these grids were analyzed with a *Philips 208* electron microscope at a 100 kV voltage, and the resulting images were collected with an *AMT* high-resolution digital imaging camera. All the high-resolution TEM images were obtained from the deposition onto lacey C grids of dispersions (approximately 1 mg ml^{-1}) of ***ox*-DWCNTs** in 1,2-dichlorobenzene; these grids were analyzed with a *F. E. I. Tecnai F20* electron microscope operating at 200 kV equipped with a Schottky type electron emitter. TM-AFM measurements were carried out in air at 298 K, using a *Nanoscope IIIa* (Digital instruments Metrology Group, USA) instrument, model: MMAFMLN. The tips used in all measurements were phosphorous-doped silicon cantilevers (T = 20–80 nm, L = 115.135 mm, f_0 = 200–400 kHz, k = 20–80 N m^{-1}, *VEECO*, USA) at a resonance frequency of ca. 316 kHz. 1–2 Drops from dispersions in 1,2-dichlorobenzene (less than 1 mg ml^{-1}) of pristine CNTs (both types), ***sh*-CNTs**, and ***ox*-CNTs** were spin-coated (spinning rate: 2000 rpm) on clean Si(1 1 1) surfaces; the silicon substrates were previously cleaned using boiling 1,1́,2,2́-tetrachloroethane for 10 min, copiously rinsed with acetone, then dried with a N_2 stream. Micro-Raman measurements were performed with an *inVia Renishaw* spectrometer, equipped with a

Samsung Ex. 1011, Page 2 of 8
Samsung Electronics Co., Ltd., et al. v. Molecular Rebar Design, LLC
IPR2025-00358

633 nm laser source using a 50× objective and power below 1 mW. Samples were prepared pressing them on a KBr disk.

2.3. *Lengths evaluation*

The statistical treatment was carried out on samples containing **ox-CNTs**. The data files collected with the AFM instrumentation were analyzed with WSxM 2.1 (Nanotec Electronica, Spain) software, in order to generate image files containing the samples topology. The criteria adopted for the discrimination between isolated and bundled **ox-CNTs** will be discussed below.

2.4. *Statistical analysis*

The length values obtained after the AFM characterization and evaluation were analyzed with the statistics tools of Origin Pro (version 7.0383), in order to obtain the frequency count necessary to draw the plots reported in Fig. 6, and the descriptive statistic values, such as the mean, the standard deviation, the standard error of the mean, the lower, intermediate and upper quartiles (P25, P50 and P75).

3. Results and discussion

Starting from CNT samples, containing DWCNTs and a certain fraction of Vt-MWCNTs, uncappened and shortened CNTs have been obtained in a two-step oxidative treatment, as displayed in Fig. 1. The first step consists in a wet oxidation reaction using H_2O_2 (15%), which mainly causes the uncapping of the tube ends and the shortening of the CNT's length *via* oxidative attack on the defects present on their sidewalls (***sh*-CNTs**, constituted of ***sh*-DWCNTs** and ***sh*-Vt-MWCNTs**). After acidic wash, necessary to remove the residual oxidized catalyst particles and other carbonaceous material, ***sh*-CNTs** with a good purity were obtained, with yields ranging from ~48% (from the 2100 grade) to ~66% (from the further purified 2101 grade). In the second step, a heat treatment (at 450 °C for 45 min under an external air purge) has been carried out with the aim of maximizing the CNT tip destruction and further reducing the content of amorphous carbonaceous material (***ox*-CNTs**, constituted of ***ox*-DWCNTs** and ***ox*-Vt-MWCNTs**). We cannot exclude that during this step a further moderate shortening of the nanotubes could happen, as reported in literature when similar conditions were applied onto SWCNTs using different combinations of temperature and time [43,44]. As expected, no major differences have been found using 2100 and 2101 grade CNTs, a part the overall yields after the two oxidations, which revealed to be 23% and 42 w/w for the 2100 and 2101 grade CNTs, respectively.

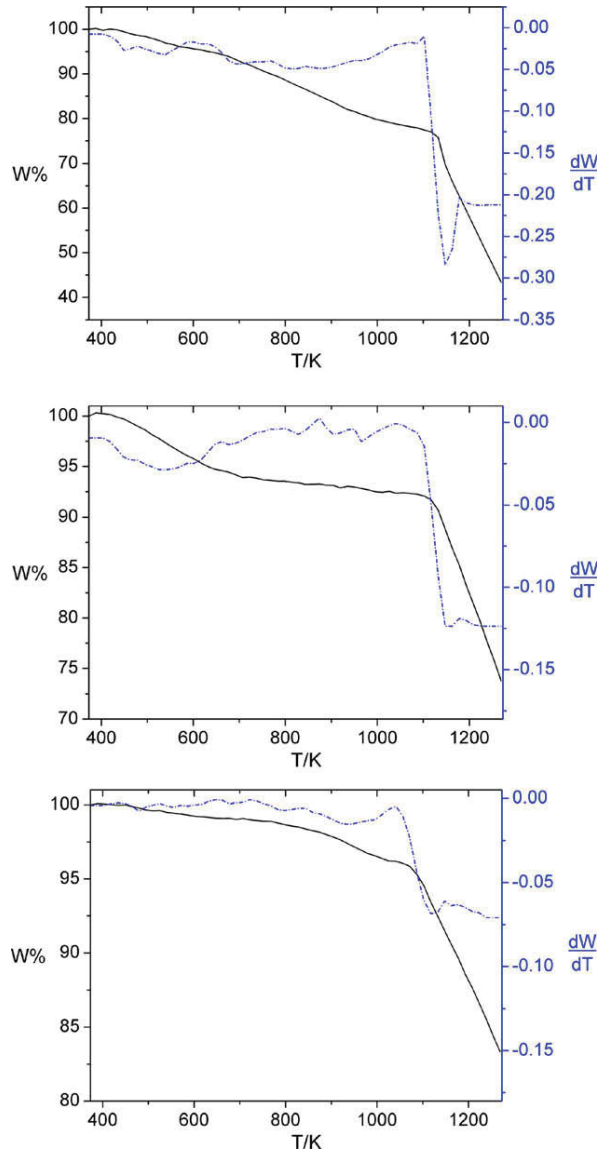

Fig. 2 – Thermogravimetric traces (——) for *pristine*-CNTs (0.770 mg, top graph), *sh*-CNTs (0.924 mg, mid graph) and *ox*-CNTs (1.608 mg, bottom graph). The abridged weight loss of *sh*-CNTs and *ox*-CNTs shows a dramatic decrease of the impurity content in the sample after the oxidizing treatments. Differential thermogravimetric plots (- - -), underlying the temperature ranges of decompositions.

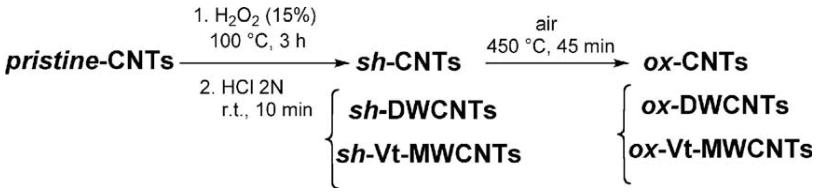

Fig. 1 – Schematic representation of the reaction conditions employed in our two-step mild oxidative protocol.

Samsung Ex. 1011, Page 3 of 8
Samsung Electronics Co., Ltd., et al. v. Molecular Rebar Design, LLC
IPR2025-00358

3.1. *Thermogravimetric analysis*

Thermogravimetric analysis [47–49] has been used as first technique to characterize the ***sh*-CNT** and ***ox*-CNT** samples; the analytical data are reported as temperature modulated and differential thermogravimetric plots (Fig. 2).

Fig. 2 displays the sudden weight loss of both ***ox*-CNTs** and ***sh*-CNTs** with respect to the pristine samples, due to the compositional changes occurred during the progressive mild-oxidation: the differential thermal plots, Fig. 2b, shows three distinct temperature ranges in which the CNT materials decompose. In the range between 400 and 625 K, one can measure the weight loss mainly caused by the pirolysis of the carboxylic groups; as can be observed (5% of weight loss, approximately 1.14 μmol COOH·mg^{-1}), both ***pristine*-CNTs** and ***sh*-CNTs** seem to possess similar content of COOH functionalities, due to the mild oxidative conditions of the first step. The second oxidation step (air purge at 673 K) has confirmed the further decrease of the carboxylic groups content in the ***ox*-CNT** samples: the reduction of the carboxylated carbonaceous fragments (CCFs) and of the simple decarboxylation process, the weight loss till 625 K is limited to 1.4% (0.32 μmol COOH per mg). In the temperature range between 650 and 1050 K only the pristine samples show a relevant weight loss (17%) that is probably associated to the decomposition of metallic and carbonaceous impurities, the presence of which is limited in the oxidized samples (6.5% and 3% for ***sh*-CNTs** and ***ox*-CNTs**, respectively) as also suggested by the Raman observations. At last, the decomposition temperatures, occurring in the range between 1125 and 1150 K, appear to be similar for all the three materials.

3.2. *Raman spectroscopy*

By analyzing the Raman spectra, one can obtain information about the type of nanotubes present in a sample and their defects and about the presence of other impurities [50]. Defects and impurities of carbon origin are usually understood on the basis of the D-band at about 1330 cm^{-1}, the intensity of which is related to their concentration [51]. The type of nanotubes can be recognized, on the other hand, from the radial breathing mode (RBM) vibrations, found below 400 cm^{-1}. The frequencies of these vibrations are proportional to the inverse of the diameter of the nanotubes and can also be used, considering the resonance condition for recording the spectrum, to obtain information about the chiral numbers of individual nanotubes [51,52]. It is of particular interest, especially for DWCNTs, to distinguish the RBM of nanotubes which are internal and external. Considering that the diameter of nanotubes was found to be larger than about 0.6 nm and that the difference in diameter between internal and external nanotubes is about 0.68–0.72 nm, one can conclude that vibrations which are above 190–200 cm^{-1} can be assigned to internal walls. The Raman spectra of ***pristine*-**, ***sh*-**, and ***ox*-CNT** materials, recorded using the 633 nm laser line of a He–Ne laser, are reported in Fig. 3. All spectra have been normalized using the G-band at 1588 cm^{-1}. We can observe in Fig. 3a that the D-band shows a decreasing intensity after the shortening process with H_2O_2 and a further decrease after the oxidizing processes in air. Since the shortening and oxidizing processes introduce defects in the nanotube structure and, therefore, should increase the intensity of the D-band, its smaller intensity shows that these processes also operated a cleaning of the samples from carbon impurities (inset Fig. 3a). This is in accord with the data obtained from TGA measurements, which clearly show an enhancement of the purity after the oxidative treatments. In Fig. 3b, the Raman spectra variations in the RBM spectral region are also reported. In particular it can be observed a clear decreasing of the intensity of those RBM modes with frequencies at 210–220 cm^{-1}. Since the spectra were excited at 633 nm, the decrease of the RBM bands intensities accounts for a preferential reaction of metallic CNTs [53] and also shows that internal nanotubes (bands above 190–200 cm^{-1}) are attacked in contrast to what has been observed with a permanganate oxidation of DWCNTs which preserved the internal nanotubes [54]. In the present case the variation of the RBM bands are consistent with the shortening of the nanotubes which implies attacking of both external and internal nanotubes. The different reaction

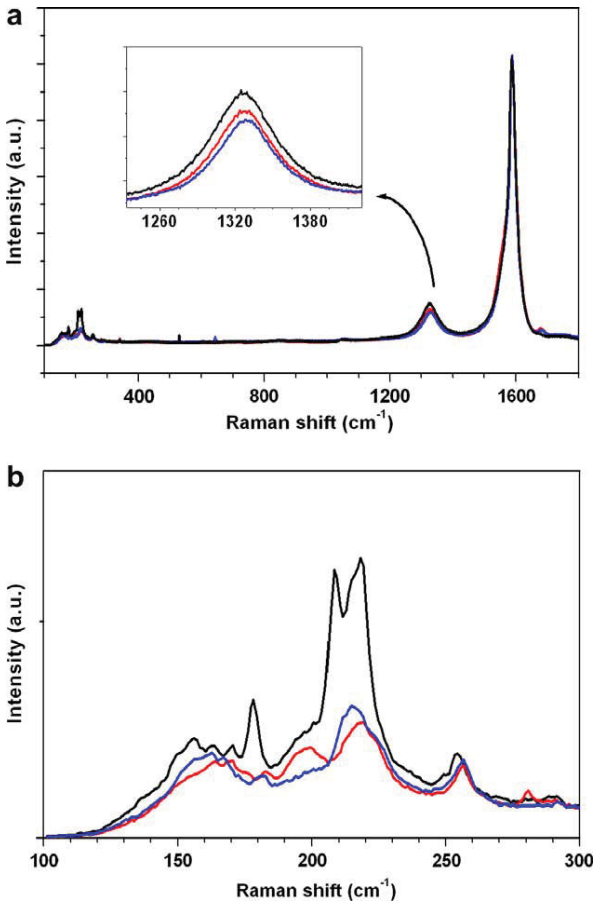

Fig. 3 – Raman spectra of *pristine*-CNTs (black line), *sh*-CNTs (red line) and *ox*-CNTs (blue line) using laser exciting line at 633 nm; insert in (a) is an expansion of the spectrum where the D-band appears; in (b) the RBM spectral region is reported. All spectra are normalized to the G-band at 1588 cm^{-1}. (For interpretation of the references to colour in this figure legend, the reader is referred to the web version of this article.)

Samsung Ex. 1011, Page 4 of 8
Samsung Electronics Co., Ltd., et al. v. Molecular Rebar Design, LLC
IPR2025-00358

behaviour can be related to the mechanism of oxidation of permanganate which is sterically more hindered and can be less effective for the internal walls than for the external ones.

3.3. *Microscopy characterization*

All DWCNTs samples were also investigated by means of TEM microscopy. TEM analysis has been carried out in order to evaluate at first the purity [55] of the samples (on the basis of the aspect of the collected images) and, in a second step (by means of high-resolution microscopes), the successful uncapping and shortening. The low magnification TEM images of ***pristine***- and ***ox***-CNTs are shown in Fig. 4a and b, respectively. As it clearly appears, unambiguous differences in the images taken before and after the oxidative treatment are displayed: picture (a) shows bundles of long and some less aggregated DWCNTs and Vt-MWCNTs as the most representative species in the pristine samples. On the other hand, after the oxidation, the average length and the aggregation level of the nanotubes have been clearly reduced (picture (b)). With regard to the purity issue, we only found minor differences between the ***ox*-CNTs** and ***pristine*-CNTs**, accounting for a high level of purity of the starting sample of CNTs.

In order to further demonstrate the effectiveness of our mild method to shorten and cut the CNT tips, the changes on the individual structure of the ***ox*-DWCNTs** have been observed with high-resolution TEM imaging. We were also able to observe many tips of isolated and bundled nanotubes. As a consequence of the oxidation reaction, the majority of the terminations were found to be opened. In particular, open ends were mostly associated at the isolated nanotubes, while in the CNT bundles, partially opened and close tips were found. In the above image of Fig. 5, an ***ox*-DWCNTs** open end is displayed (a), in which the related inner cavity, as in many other cases, is partially filled with a carbonaceous material (b). These observations further confirm the feasibility of the insertion, after previous removal of the inner carbonaceous material, of molecular species inside the inner cavities of these opened DWCNTs.

In the literature, several papers report the ability to purify (and/or shorten) SWCNTs, but a few of them clearly report a detailed structural analysis, i.e., lengths and diameters [33,43,44,56–62]. This structural aspect is very important because, on the basis of the length distribution of the CNT content, the materials' physico-chemical and mechanical properties are changing, thus dramatically affecting their applicability in specific functional materials. In order to evaluate the effectiveness of the employed oxidizing conditions on the shortening reaction, a statistical evaluation of the CNTs' length as measured by AFM, is reported.

By means of AFM imaging in the tapping mode, we have analyzed several samples of ***ox*-CNTs**, in which the oxidized

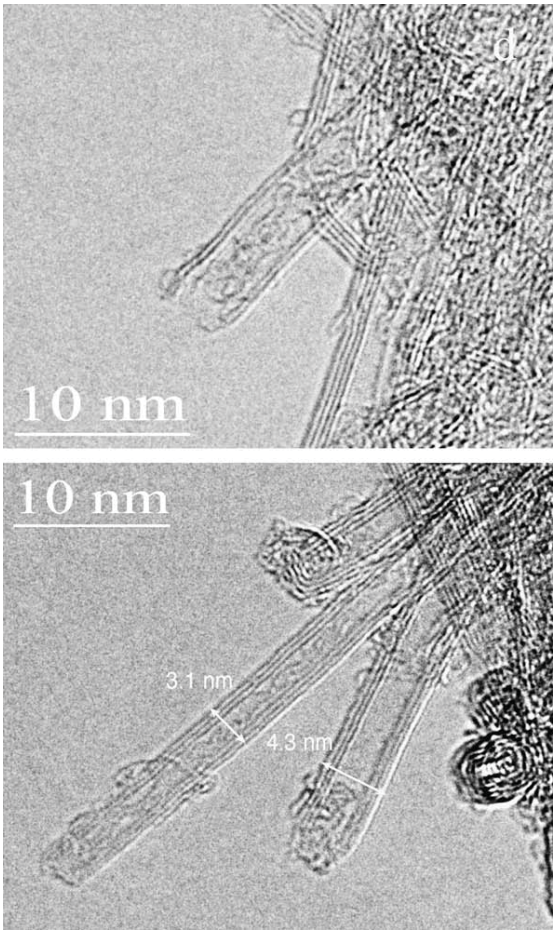

Fig. 5 – HR-TEM micrograph images of an *ox*-DWCNT (above) and of an *ox*-Vt-MWCNT (below) deposited on Cu grids with lacey carbon film, showing open nanotube tips (a) and the material present in the inner cavity (b).

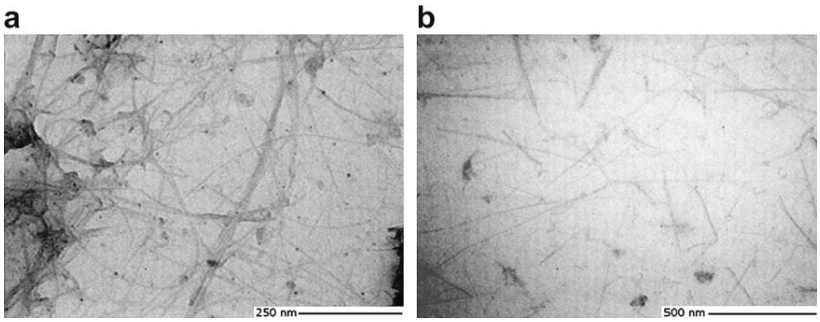

Fig. 4 – Low magnification TEM micrographs images deposited on Cu grids coated with a carbon film, showing long bundled and isolated CNTs (picture (a), pristine sample) and shortened, less aggregated nanotubes *ox*-CNTs, picture (b).

Samsung Ex. 1011, Page 5 of 8
Samsung Electronics Co., Ltd., et al. v. Molecular Rebar Design, LLC
IPR2025-00358

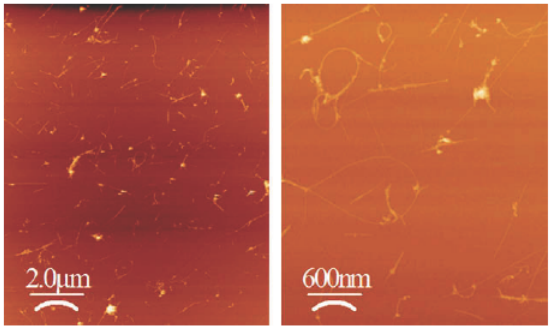

Fig. 6 – Tapping mode AFM images (scan size of 10 (left) and 3 μm (right)) at 298 K of *ox*-CNTs deposited on clean Si (111) surface.

material was deposited on Si(111) surfaces by spin-coating a dispersion of ***ox*-CNTs** in 1,2-dichlorobenzene. Due to the low tendency to aggregate, all nanotubes dispersed very well in such solvent, facilitating the preparation of many reproducible samples and the collection of several images containing several individual CNTs, as those depicted in the images of Fig. 6.

Using WSxM 2.1 (Nanotec Electronica, Spain) software, the objects found on the silicon surface were analyzed through the evaluation of their cross section. Depending on the diameters values reported by the CNT manufacturer (average = 3.5 nm) and considering the deconvolution of the AFM tip, we have classified the observed objects in two groups: all the measured diameter values smaller than 7 nm have been associated to isolated ***ox*-DWCNTs** or ***ox*-Vt-MWCNTs**, whereas all values greater than 7 nm have been correlated to bundled or very thick MWCNTs. Only those objects classified as isolated nanotubes (a total of 400 units) were measured in their lengths, to give the basis for a set of values being subjected to the statistical treatment (Table 1).

On the basis of manufacturer's datasheet, the length values of the ***pristine*-CNTs** can vary from 1 to 10 μm. After the shortening treatment, both weighted and arithmetical means possesses similar values, respectively, of 534.13 and 537.19 nm, with a correlated standard deviation of 377.35 nm. Over the 400 counted objects, 383 tubes were shorter than 1 μm, and only a narrow number were longer than 1.5 or 2 μm, with the latter values severely affecting the standard deviation. In the frequency count diagram (Fig. 7a), the upper quartile has a value slightly greater than those of the calculated means, thus indicating that the 75% of the AFM-observed CNTs are shorter than 710 nm. The information reported in Table 1 became thus clearer if associated with the frequency histograms depicted in Fig. 7a, where the frequencies of the observed lengths have been plotted as functions of the different dimensional classes. In plot (a) the length distribution of the analyzed ***ox*-CNT** materials is reported as functions of the length's dimensional classes, showing a bimodal course; as reported in the statistical results summarized in Table 1, the most frequent lengths falls in the dimensional classes from 200 to 400 nm. In plot (b)

Table 1 – Results of the statistical analysis on the 400 length values obtained from the AFM analysis, expressed in nanometers. $\bar{x}$ and $\bar{x}_w$ represents the arithmetic and the weighted means, respectively; σ and μ_m are the standard deviations and the standard error of the mean, respectively; Q_1, Q_2, and Q_3 are the lower, median, and upper quartiles, respectively.

$\bar{x}$	$\bar{x}_w$	σ	μ_m	Q_1	Q_2	Q_3
537.19	534.13	377.35	18.87	275.70	398.53	710.81

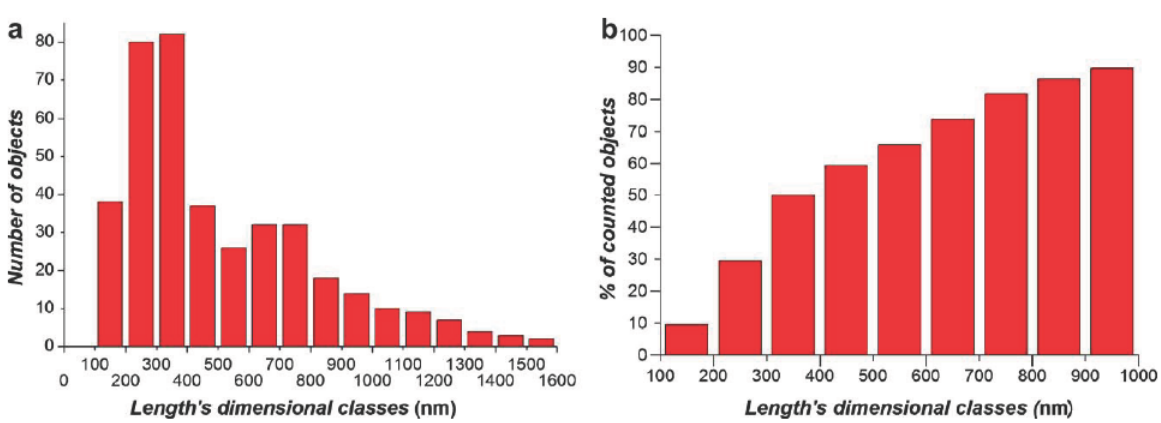

Fig. 7 – Frequency (a) and cumulative percentage (b) curves of the AFM measured *ox*-CNTs, as functions of the length's dimensional classes. Plot (a) shows the observed bimodal length's distribution, in which the most frequent length values are comprised between 200 and 400 nm. Plot (b) illustrates that half of *ox*-CNTs fall in the range from 100 to 500 nm, and 90% of them are shorter than 1 μm.

Samsung Ex. 1011, Page 6 of 8
Samsung Electronics Co., Ltd., et al. v. Molecular Rebar Design, LLC
IPR2025-00358

the cumulative frequency histograms illustrate that the 90% of the measured objects falls in dimensional classes associated at length values shorter than 1 μm.

4. Conclusions

In every oxidizing process there is a balance between catalyst removal (if present), total loss of the CNT content, shortening of the tubes, and amount of carboxylic moieties onto their tips and sidewalls. This balance is affected by several parameters, like the properties of the pristine samples, kind and strength of the oxidizing agents, time and temperature of the reaction. All the analytical and statistical results discussed in this report unambiguously confirm that the mild oxidative conditions employed in this work controllably shorten the CNTs's length. We have shown that the employed mild oxidizing agent (H_2O_2 15% solution) and the reaction conditions (100 °C for 3 h) here described represent a better synthetic path toward controlled shortening and uncapping of DWCNTs and Vt-MWCNTs since stronger oxidizing protocols (e.g., HNO_3 and H_2SO_4) are known to dramatically reduce the materials quantity. By means of HR-TEM, we have also demonstrated that most of the shortened CNTs are opened at their tips, thus making their inner cavity accessible towards any potential guest.

Acknowledgements

This work was supported by the European Union through the Marie-Curie Research Training Network "PRAIRIES", Contract MRTN-CT-2006-035810, Marie-Curie Initial Training Network "FINELUMEN", Grant agreement PITN-GA-2008-215399, the University of Trieste, INSTM, MUR (PRIN 2006, Prot. 2006034372 and FIRB, Prot. RBIN04HC3S), and the University of Namur.

REFERENCES

[1] Iijima S. Helical microtubules of graphitic carbon. Nature 1991;354(6348):56–8.
[2] Iijima S, Ichihashi T. Single-shell carbon nanotubes of 1 nm diameter. Nature 1993;363(6430):603–5.
[3] Bethune DS, Kiang CH, de Vries MS, Gorman G, Savoy R, Vazquez J, et al. Cobalt-catalyzed growth of carbon nanotubes with single-atomic-layerwalls. Nature 1993;363(6430):605–7.
[4] Lahr B, Sandler J. Carbon nanotubes – high-strength reinforcing compounds for composites. Kunststoffe-Plast Europe 2000;90(1):A94–A100.
[5] Guldi DM. Materials science – nanotubes see the light. Nature 2007;447(7140):50–1.
[6] Guldi DM, Rahman A, Sgobba V, Ehli C. Multifunctional molecular carbon materials – from fullerenes to carbon nanotubes. Chem Soc Rev 2006;35(5):471–87.
[7] Sgobba V, Guldi DM. Carbon nanotubes as integrative materials for organic photovoltaic devices. J Mater Chem 2008;18(2):153–7.
[8] White CT, Todorov TN. Quantum electronics – nanotubes go ballistic. Nature 2001;411(6838):649–51.
[9] Long RQ, Yang RT. Carbon nanotubes as a superior sorbent for nitrogen oxides. Ind Eng Chem Res 2001;40(20):4288–91.
[10] Bianco A, Prato M. Can carbon nanotubes be considered useful tools for biological applications? Adv Mater 2003;15(20):1765–8.
[11] Bradbury J. Beyond pills and jabs – researchers develop new ways to get drugs to the right place at the right time. Lancet 2003;362(9400):1984–5.
[12] Allen TM, Cullis PR. Drug delivery systems: entering the mainstream. Science 2004;303(5665):1818–22.
[13] Martin CR, Kohli P. The emerging field of nanotube biotechnology. Nat Rev Drug Discov 2003;2(1): 29–37.
[14] Cai H, Cao XN, Jiang Y, He PG, Fang YZ. Carbon nanotube-enhanced electrochemical DNA biosensor for DNA hybridization detection. Anal Bioanal Chem 2003;375(2):287–93.
[15] Gooding JJ, Wibowo R, Liu JQ, Yang WR, Losic D, Orbons S, et al. Protein electrochemistry using aligned carbon nanotube arrays. J Am Chem Soc 2003;125(30):9006–7.
[16] Patolsky F, Weizmann Y, Willner I. Long-range electrical contacting of redox enzymes by SWCNT connectors. Angew Chem Int Ed 2004;43(16):2113–7.
[17] Wang J, Liu GD, Jan MR. Ultrasensitive electrical biosensing of proteins and DNA: Carbon-nanotube derived amplification of the recognition and transduction events. J Am Chem Soc 2004;126(10):3010–1.
[18] Williams KA, Veenhuizen PTM, de la Torre BG, Eritja R, Dekker C. Nanotechnology – carbon nanotubes with DNA recognition. Nature 2002;420(6917):761.
[19] Mitchell DT, Lee SB, Trofin L, Li NC, Nevanen TK, Soderlund H, et al. Smart nanotubes for bioseparations and biocatalysis. J Am Chem Soc 2002;124(40):11864–5.
[20] Kam NWS, Dai H. Carbon nanotubes as intracellular protein transporters: generality and biological functionality. J Am Chem Soc 2005;127(16):6021–6.
[21] Pantarotto D, Singh R, McCarthy D, Erhardt M, Briand JP, Prato M, et al. Functionalized carbon nanotubes for plasmid DNA gene delivery. Angew Chem Int Ed 2004;43(39): 5242–6.
[22] Liu Z, Winters M, Holodniy M, Dai H. SiRNA delivery into human T cells and primary cells with carbon-nanotube transporters. Angew Chem Int Ed 2007;46(12):2023–7.
[23] Pantarotto D, Partidos CD, Graff R, Hoebeke J, Briand JP, Prato M, et al. Synthesis, structural characterization, and immunological properties of carbon nanotubes functionalized with peptides. J Am Chem Soc 2003;125(20):6160–4.
[24] Pantarotto D, Briand JP, Prato M, Bianco A. Translocation of bioactive peptides across cell membranes by carbon nanotubes. Chem Commun 2004(1):16–7.
[25] Prato M, Kostarelos K, Bianco A. Functionalized carbon nanotubes in drug design and discovery. Acc Chem Res 2008;41(1):60–8.
[26] Bottini M, Cerignoli F, Dawson MI, Magrini A, Rosato N, Mustelin T. Full-length single-walled carbon nanotubes decorated with streptavidin-conjugated quantum dots as multivalent intracellular fluorescent nanoprobes. Biomacromolecules 2006;7(8):2259–63.
[27] Accorsi G, Armaroli N, Parisini A, Meneghetti M, Marega R, Prato M, et al. Wet adsorption of a luminescent Eu(III) complex on carbon nanotubes sidewalls. Adv Funct Mater 2007;17(15):2975–82.
[28] Rowan SJ, Cantrill SJ, Cousins GRL, Sanders JKM, Stoddart JF. Dynamic covalent chemistry. Angew Chem Int Ed 2002;41(6):898–903.
[29] Thess A, Lee R, Nikolaev P, Dai H, Petit P, Robert J, et al. Crystalline ropes of metallic carbon nanotubes. Science 1996;273(5274):484–8.

Samsung Ex. 1011, Page 7 of 8
Samsung Electronics Co., Ltd., et al. v. Molecular Rebar Design, LLC
IPR2025-00358

[30] Amelinckx S, Zhang XB, Bernaerts D, Zhang XF, Ivanov V, Nagy JB. A formation mechanism for catalytically grown helix-shaped graphite nanotubes. Science 1994;265(5172):635–9.
[31] Nikolaev P, Bronikowski MJ, Bradley RK, Rohmund F, Colbert DT, Smith KA, et al. Gas-phase catalytic growth of single-walled carbon nanotubes from carbon monoxide. Chem Phys Lett 1999;313(1–2):91–4.
[32] Tasis D, Tagmatarchis N, Bianco A, Prato M. Chemistry of carbon nanotubes. Chem Rev 2006;106:1105–36.
[33] Liu J, Rinzler AG, Dai HJ, Hafner JH, Bradley RK, Boul PJ, et al. Fullerene pipes. Science 1998;280(5367):1253–6.
[34] Wiltshire JG, Khlobystov AN, Li LJ, Lyapin SG, Briggs GAD, Nicholas RJ. Comparative studies on acid and thermal based selective purification of HiPCO produced single-walled carbon nanotubes. Chem Phys Lett 2004;386(4–6):239–43.
[35] Sun XG, Zeng XS. An investigation on the purification of multiwall carbon nanotubes by oxidation in air. New Carbon Mater 2004;19(1):65–8.
[36] Smith MR, Hedges SW, LaCount R, Kern D, Shah N, Huffman GP, et al. Selective oxidation of single-walled carbon nanotubes using carbon dioxide. Carbon 2003;41(6):1221–30.
[37] Sen R, Rickard SM, Itkis ME, Haddon RC. Controlled purification of single-walled carbon nanotube films by use of selective oxidation and near-IR spectroscopy. Chem Mater 2003;15(22):4273–9.
[38] Martinez MT, Callejas MA, Benito AM, Cochet M, Seeger T, Anson A, et al. Modifications of single-wall carbon nanotubes upon oxidative purification treatments. Nanotechnology 2003;14(7):691–5.
[39] Lafi L, Cossement D, Chahine R. Raman spectroscopy and nitrogen vapour adsorption for the study of structural changes during purification of single-wall carbon nanotubes. Carbon 2005;43(7):1347–57.
[40] Chikkannanavar SB, Luzzi DE, Paulson S, Johnson AT. Synthesis of peapods using substrate-grown SWNTs and DWNTs: an enabling step toward peapod devices. Nano Lett 2005;5(1):151–5.
[41] Zhang XF, Cao AY, Sun QH, Xu CL, Wu DH. Oxidation and opening of well-aligned carbon nanotube tips. Mater Trans 2002;43(7):1707–10.
[42] Khlobystov AN, Britz DA, Andre G, Briggs D. Molecules in carbon nanotubes. Acc Chem Res 2005;38(12):901–9.
[43] Ziegler KJ, Gu ZN, Shaver J, Chen ZY, Flor EL, Schmidt DJ, et al. Cutting single-walled carbon nanotubes. Nanotechnology 2005;16(7):S539–44.
[44] Ziegler KJ, Gu Z, Peng H, Flor EL, Hauge RH, Smalley RE. Controlled oxidative cutting of single-walled carbon nanotubes. J Am Chem Soc 2005;127(5):1541–7.
[45] Bonifazi D, Nacci C, Marega R, Campidelli S, Ceballos G, Modesti S, et al. Microscopic and spectroscopic characterization of paintbrush-like single-walled carbon nanotubes. Nano Lett 2006;6(7):1408–14.
[46] Dillon AC, Parilla PA, Alleman JL, Gennett T, Jones KM, Heben MJ. Systematic inclusion of defects in pure carbon single-wall nanotubes and their effect on the Raman D-band. Chem Phys Lett 2005;401(4–6):522–8.
[47] Bom D, Andrews R, Jacques D, Anthony J, Chen BL, Meier MS, et al. Thermogravimetric analysis of the oxidation of multiwalled carbon nanotubes: evidence for the role of defect sites in carbon nanotube chemistry. Nano Lett 2002;2(6):615–9.
[48] McKee GSB, Vecchio KS. Thermogravimetric analysis of synthesis variation effects on CVD generated multiwalled carbon nanotubes. J Phys Chem B 2006;110(3):1179–86.
[49] Landi BJ, Cress CD, Evans CM, Raffaelle RP. Thermal oxidation profiling of single-walled carbon nanotubes. Chem Mater 2005;17(26):6819–34.
[50] Dresselhaus MS, Dresselhaus G, Avouris P, editors. Carbon nanotubes, synthesis, structure, and applications. Berlin Heidelberg: Springer-Verlag; 2001.
[51] Kataura H, Kumazawa Y, Kojima N, Umezu I, Masubuchi S, Kazama S, et al. Optical properties of single-wall carbon nanotubes. Synth Met 1999;103:2555–8.
[52] Maultzsch J, Telg H, Reich S, Thomsen C. Radial breathing mode of single-walled carbon nanotubes: optical transition energies and chiral-index assignment. Phys Rev B 2005;72(20):205438.1–16.
[53] Menna E, Della Negra F, Dalla Fontana M, Meneghetti M. Selectivity of chemical oxidation attack of single-wall carbon nanotubes in solution. Phys Rev B 2003;68(19):193412.1–4.
[54] Marcolongo G, Ruaro G, Gobbo M, Meneghetti M. Amino acid functionalization of double-wall carbon nanotubes studied by Raman spectroscopy. Chem Commun 2007(46): 4925–7.
[55] Kitiyanan B, Alvarez WE, Harwell JH, Resasco DE. Controlled production of single-wall carbon nanotubes by catalytic decomposition of CO on bimetallic Co-Mo catalysts. Chem Phys Lett 2000;317:497–503.
[56] Vieira HS, Andrada DM, Mendonca R, Santos AR, Martins MD, Macedo WAA, et al. Decarboxylation of oxidized single-wall carbon nanotubes. J Nanosci Nanotechnol 2007;7(10):3421–30.
[57] Trigueiro JPC, Silva GG, Lavall RL, Furtado CA, Oliveira S, Ferlauto AS, et al. Purity evaluation of carbon nanotube materials by thermogravimetric, TEM, and SEM methods. J Nanosci Nanotechnol 2007;7(10):3477–86.
[58] Ziegler KJ, Schmidt DJ, Rauwald U, Shah KN, Flor EL, Hauge RH, et al. Length-dependent extraction of single-walled carbon nanotubes. Nano Lett 2005;5(12):2355–9.
[59] Xu YQ, Peng HQ, Hauge RH, Smalley RE. Controlled multistep purification of single-walled carbon nanotubes. Nano Lett 2005;5(1):163–8.
[60] Furtado CA, Kim UJ, Gutierrez HR, Pan L, Dickey EC, Eklund PC. Debundling and dissolution of single-walled carbon nanotubes in amide solvents. J Am Chem Soc 2004;126(19):6095–105.
[61] Edelmann FT. Fullerene pipes, tube-in-tube membranes, and carbon-nanotube tips: adding new dimensions to molecular technology. Angew Chem Int Ed 1999;38(10):1381–7.
[62] Venkateswaran UD, Masica DL, Sumanasekera GU, Furtado CA, Kim UJ, Eklund PC. Diameter dependent wall deformations during the compression of a carbon nanotube bundle. Phys Rev B 2003;68(24):241406–9.

Samsung Ex. 1011, Page 8 of 8
Samsung Electronics Co., Ltd., et al. v. Molecular Rebar Design, LLC
IPR2025-00358